Stem Cell Research 28 (2018) 75–86

Contents lists available at ScienceDirect

Stem Cell Research

journal homepage: www.elsevier.com/locate/scr

Exposure to the ROCK inhibitor fasudil promotes gliogenesis of neural stem cells *in vitro*

Zubair Ahmed Nizamudeen [a], Lisa Chakrabarti [b], Virginie Sottile [a,*]

[a] Wolfson STEM Centre, School of Medicine, University of Nottingham, UK
[b] School of Veterinary Science, University of Nottingham, UK

ARTICLE INFO

Article history:
Received 6 December 2017
Received in revised form 30 January 2018
Accepted 2 February 2018
Available online 6 February 2018

Keywords:
Fasudil
ROCK inhibitor
Neural stem cells
Differentiation
Gliogenesis
Primary cultures

ABSTRACT

Fasudil is a clinically approved Rho-associated protein kinase (ROCK) inhibitor that has been used widely to treat cerebral consequences of subarachnoid hemorrhage. It is known to have a positive effect on animal models of neurological disorders including Parkinson's disease and stroke. However, its cellular effect on progenitor populations and differentiation is not clearly understood. While recent studies suggest that fasudil promotes the mobilization of neural stem cells (NSCs) from the subventricular zone *in vivo* and promotes the differentiation of the C17.2 cerebellar neuroprogenitor line *in vitro*, it is unclear whether fasudil is involved in the differentiation of primary NSCs.

Here, we tested the effect of fasudil on mouse NSCs *in vitro*, and observed increased gliogenesis in NSCs derived from lateral ventricles. Upon treatment, fasudil promoted characteristics of neurogenesis including phenotypic changes in neural outgrowth and interkinetic nuclear-like movements as an immediate response, while Sox2 expression was maintained and GFAP expression increased. Moreover, the gliogenic response to fasudil medium was observed in both early postnatal and adult NSC cultures.

Taken together, our results show that fasudil promotes the differentiation of NSCs into astroglial lineage, suggesting that it could be used to develop novel vitro gliogenesis models and regulate differentiation for neural repair.

1. Introduction

Fasudil is a ROCK inhibitor that has been shown to alleviate symptoms from a range of CNS disorders including subarachnoid hemorrhage, spinal cord injuries, cerebral stroke, Parkinson's disease, neuropathic pain and epilepsy (Chen et al., 2013; Nakamura et al., 2013; Satoh et al., 2012; Hara et al., 2000; Baba et al., 2010; Impellizzeri et al., 2012; Wang et al., 2012; Mueller et al., 2005; Shibuya et al., 1992; Villar-Cheda et al., 2012; Boyce-Rustay et al., 2010; Inan and Büyükafşar, 2008). Although other ROCK inhibitors including C3 transferase and Y27632 have shown similar neurogenic effects on animal models *in vivo* and *in vitro*, fasudil is the only clinically approved ROCK inhibitor currently in use for patients suffering from CNS disorders (Jia et al., 2016; Gu et al., 2013).

Accumulation of Rho-associated protein kinase (ROCK) has been involved in a variety of neuronal functions including inhibition of axonal regeneration, inhibition of neuronal differentiation and proliferation of tumor cells (Chen et al., 2013; Liu et al., 2015; Compagnucci et al., 2016; Ying et al., 2006). ROCK is a direct downstream effector of Rho, a member of the Rho-GTPases belonging to the Ras superfamily (Liu et al., 2015). There are two isoforms of ROCK – ROCK1 and ROCK2, of which the latter is mainly expressed in the central nervous system. Myelin-associated inhibitory factors such as myelin associated glycoprotein, oligodendrocyte myelin glycoprotein and Nogo can activate the Rho-ROCK signaling pathway by binding to the Nogo receptor/Lingo-1/p75 receptor complex present in the cell membrane (Liu et al., 2015). Activated ROCK can then phosphorylate the myosin light chain which leads to a series of events that causes neurite retraction and collapse of the growth cone in the central nervous system (Liu et al., 2015). The result is a lack of nerve growth, neural support and axon regeneration. Therefore, inhibitors for Rho-ROCK pathway are being targeted for their potential to treat neurological disorders (Chen et al., 2013).

An *in vivo* study has shown that intra peritoneal administration of fasudil in a hypoxia/reoxygenation mouse model can mobilize endogenous progenitors from the SVZ, suggesting that NSCs may be fasudil-responsive (Ding et al., 2010). Moreover, a recent study reported that fasudil could differentiate the cerebellum-derived C17.2 neural cell line into neurons and glia *in vitro*. However the cellular effects of this drug on neuroprogenitor cell populations remain unclear and there has been no study on the response to fasudil in primary NSC cultures *in vitro*. Here, we analysed the effect of fasudil on primary NSC culture

* Corresponding author.
E-mail address: virginie.sottile@nottingham.ac.uk (V. Sottile).

https://doi.org/10.1016/j.scr.2018.02.001

and differentiation *in vitro* using cells isolated from the lateral ventricles of early postnatal and adult mouse brain tissue.

2. Methods

All reagents used were purchased from Thermofisher (UK) unless otherwise stated.

2.1. Cell culture

For primary NSC isolation, lateral ventricle tissues from postnatal day 21 and adult mice brain were isolated from lateral ventricle tissue, which was carefully dissected from coronal sections immersed in PBS, transferred to a new dish to be briefly minced, and then transferred to a conical tube containing Accumax (Sigma-Aldrich, UK) for 30 min at 37 °C, with mild agitation every 10 min. The digested tissues were then washed with PBS and centrifuged at 200*g* for 5 min. The cell pellet was re-suspended in NSC medium (made from DMEM F12/Neurobasal (1:1) medium containing 0.5% Penicillin/Streptomycin (P/S) and 0.01% heparin, with B27 and N2 supplements, and added growth factors bFGF and EGF (20 ng/μl)). The cells were split using Accutase (Sigma-Aldrich, UK) and used within 10 passages. For differentiation, postnatal NSCs were seeded on 0.1% gelatin coated coverslips at 50,000 cells/ml (Adult LV-NSCs were seeded on Geltrex to reduce cell loss during immunostaining washes). Upon reaching confluency, the medium was changed to differentiation medium (identical to NSC medium but without growth factors), supplemented with 0.05% FCS, with or without 100 μM Fasudil (FAS, Tocris) as indicated. For neuronal differentiation, the differentiation medium without Fasudil was supplemented with the retinoic acid analogue 1 μM EC23 (Tocris) and 10 ng/μl BDNF (Source Bioscience) which was referred to as retinoid-based medium (RET).

C17.2 immortalised mouse cerebellar cells were cultured in DMEM high glucose medium supplemented with 10% FCS and 0.5% P/S. This cell line was used as a positive control for fasudil mediated neuronal differentiation *in vitro* (Chen et al., 2015). For differentiation, C17.2 cells were seeded onto coverslips placed at 40,000 cells/ml. After 24 h, the medium was refreshed and supplemented with 100 μM FAS.

2.2. Neurite outgrowth analysis

Images of undifferentiated and FAS-treated cultures were captured using Nikon microscope and images processed using ImageJ software (www.imagej.nih.gov/ij/). Images were captured from 3 independent biological replicates, and from each replicate 3 image sections were selected for neurite outgrowth measurements (technical replicates). Only the neurite lengths longer than the diameter of the cell body were considered for analysis. Total neurite length was normalised to the number of cells visualized in each image.

2.3. Immunohistochemistry

Cells were fixed in 4% ice-cold paraformaldehyde (PFA), washed with PBS, then incubated in 0.1% Triton-X (Sigma-Aldrich), followed by a PBS wash. Samples were then washed briefly in PBT (PBS + 0.1% Tween20 (Sigma-Aldrich)) and blocked using 5% goat serum (Sigma-Aldrich) in PBS. Samples were incubated overnight in primary antibodies diluted in blocking solution, using the following antibody dilutions: Nestin (mouse monoclonal; 1:50; Dako), Sox2 (rabbit polyclonal; 1:500; EMD Millipore), βIII-Tubulin (rabbit polyclonal; 1:1000; Abcam), GFAP (rabbit polyclonal; 1:250; Dako), S100b (1:200; Dako) and DCX (1:500; Cell Signalling). Samples were then briefly washed in PBT and incubated for 1 h in secondary antibodies diluted in blocking solution, with the following dilutions: Alexa Fluor 488-conjugated goat anti-mouse (1:250), Alexa Fluor 488-conjugated goat anti-rabbit (1:250), Alexa Fluor 594-conjugated goat anti-rabbit solution (1:20), Alexa Fluor 647-conjugated goat anti-rabbit (1:250) followed by brief PBT wash. Samples were mounted using DAPI-containing Vectashield mounting solution (Vector Laboratories, UK) and imaged with a Nikon Eclipse 90i fluorescent microscope. Alternatively, immunostained samples were incubated in DAPI solution and imaged using Operetta High-Content Imaging System (Perkin Elmer, UK). Quantitative analysis of immunofluorescence was performed using the ImageJ software (for images captured by Nikon 90i microscope) or the Harmony Image Analysis system (for images captured by Operetta). For ImageJ, immunostaining was quantified by determining the area of intensity of particular antibody fluorescence over the area covered by DAPI fluorescence for each image. Immunofluorescent quantification of samples for particular antibodies were then normalised to their respective day 0 samples. For images processed by Harmony Software, total fluorescence was calculated and averaged from 9 randomly selected fields of view per well. All quantifications were analysed above the negative threshold set calculated from negative control fluorescence.

2.4. Reverse transcriptase PCR (RT-PCR) and quantitative PCR (qPCR)

Cells were processed using TRI Reagent (Sigma-Aldrich) and total RNA extracted using RNA Clean and Concentrator (Zymo Research) following the manufacturer's protocols. DNAse 1 treatment was applied and reverse transcription (RT) was performed using 1 μg RNA with the Superscript 3 RT enzyme kit, following manufacturer's protocol. PCR was performed using the Platinum Taq DNA polymerase kit and the following primers: Clathrin6k (F: 5′-GACAGTGCCATCATGAATCC-3′, R: 5′-TTTGTGCTTCTGGAGGAAAGAA-3′), Nestin (F: 5′-AGAGTCA GATCGCTCAGATCC-3′, R: 5′-GCAGAGTCCTGTATGTAGCCAC-3′), Sox2 (F: 5′-GGCGGCAACCAGAAGAACAG-3′, R: 5′-GCTTGGCCTCGTCGA TGAAC-3′), GFAP (F: 5′-CTCAATGCTGGCTTCAAGGAG-3′, R: 5′-GG ATCTCCTCCTCCAGCGA-3′) and βIII-tub (F: 5′-GGCCTCCTCTCACAAG TATGT-3′, R: 5′-CAGGGAATCGAAGGGAGGTG-3′). Tubes containing no RNA and no enzyme controls were used in parallel reactions to confirm the absence of contamination. ImageJ software was used to calculate band intensities from gel and normalise to Clathrin6k (housekeeping gene) to provide semi-quantification of gene expression. For qPCR, Power SYBR Green PCR Master Mix (Applied Biosystems) was used. Gene expression was normalised against expression of Clathrin6k and calculated using $2-\Delta\Delta Ct$. The following primers were used: Clathrin6k (F: 5′-AGATTCTGCCCATTCGCTTTC-3′, R: 5′-TCAGTGCAATCACTT TGCTGG-3′), Nestin (F: 5′-AGAGTCAGATCGCTCAGATCC-3′, R: 5′-GCAGAGTCCTGTATGTAGCCAC-3′), Sox2 (same as mentioned above for RT-PCR), βIII-tub (F: 5′-GCGCCTTTGGACACCTATTCA-3′, R: 5′-GCCCTCCGTATAGTGCCCT-3′), GFAP (F: 5′-GAGGAGTGGTATCGGT CTAAGTTTG-3′, R: 5′-GCCGCTCTAGGGACTCGTT-3′). Primers were validated using mouse brain tissue as positive control, and mouse liver tissue as negative control. Mean gene expression ($2-\Delta\Delta Ct$) was calculated between two independent experiments with three replicates and graphed with standard deviation (SD).

2.5. Metabolic activity assay

Presto Blue (PB) kit was used to analyse the metabolic activity of differentiating cells according to manufacturer's instructions. NSCs and C17.2 cells were seeded at 50,000 and 15,000 cells per well in 24-well plates, or 5000 and 1000 cells per well in 96 well plates, respectively. To normalise presto blue fluorescence to cell numbers, cell counts were performed with ImageJ software using 3 randomly selected regions on brightfield images for each of the 3 replicate wells analysed per condition. DNA quantitation was carried out using the PicoGreen dsDNA assay (according to manufacturer's protocol). To determine the change in cell number on day 2 and day 4 FAS-treated and untreated samples, all cell count values for treated samples were normalised to the cell count of day 0 untreated samples. To determine the change in metabolic activity on day 2 and day 4 FAS-treated and untreated

samples, all cell count-normalised PB values of treated samples were normalised to the metabolic activity of day 0 untreated samples.

2.6. Cell motility analysis

Cells were cultured in 96-well plates in biological triplicates and live imaging was performed using the Operetta High-Content Imaging system with Harmony software. Live images were taken every 3 s for 2 h and 45 min from one field of view in each well in brightfield and digital phase contrast modes to enable segmentation and tracking of cells. The building blocks for analysis were as follows: Input Image - Filter Image – Find Cells – Track Objects – Calculate Kinetic Properties – Calculate Properties – Calculate Track Properties – Define Results. Digital phase contrast images were used for tracking analysis and filtering using the sliding parabola option under 'Filter Image' block. The 'Track Properties' module was used to determine 'Accumulated Distance' (normalised to track count), 'Start/End Type', 'Number of Time-points', 'Displacement', and 'Speed' parameters of the tracked cells. The percentage of cells tracked from 'BEGIN' to 'END' (B-E type) was defined as cells that could be tracked throughout all timepoints without division/fusion events or any imaging hindrance (cosmos/border). The percentage of cells tracked from 'SPLIT' to 'SPLIT' (S-S type) was defined as actively dividing cells undergoing division at least twice while being tracked. A supplementary figure explains the cell track types graphically (Supplementary Fig. 1). The accumulated distance (normalised to track count) of B-E type tracks was used to determine changes in cell migration.

2.7. Statistical analysis

All experiments were run in triplicates using separate cultures, with at least three internal repeats. Mean and SD were analysed using either GraphPad Prism or Microsoft Excel. One way ANOVA with Tukey's multiple comparison test was run to determine the statistical significance for all analysis unless otherwise specified. Statistical significance level was set for $^{*}p < 0.05$, $^{**}p < 0.01$, $^{***}p < 0.001$, $^{****}p < 0.0001$. Complete statistical data sets for all the experiments are included in a Supplementary excel sheet (Supplementary Sheet 1).

3. Results

3.1. Fasudil alters the metabolic activity and morphology of postnatal NSCs

The effect of fasudil treatment on postnatal NSCs was first analysed through metabolic activity measured of cultures over 4 days as an indication of cell health (Fig. 1A). C17.2 cells were used as a positive control for FAS mediated neural differentiation according to a recently published study (Chen et al., 2015). 100 μM FAS was seen to increase the metabolic activity of NSCs and C17.2 (Fig. 1A). In NSCs, FAS addition produced a significant and sustained increase in metabolic activity at both time points (Fig. 1A), while in C17.2 samples FAS treatment only showed a significant metabolic increase only on day 2 (Fig. 1B).

In addition, effects on cell morphology were observed upon treatment (Fig. 1). Brightfield images of FAS-treated samples at day 2 and day 4 showed cytoskeletal changes with increased neurite outgrowth in both NSCs and C17.2 cells, compared to day 0 controls (Fig. 1C). Total neurite length increased significantly from day 2 to day 4 of FAS treatment for both cell types, and this increase was more pronounced in C17.2 cells (Fig. 1D). We noticed that NSCs showed smooth radial-like elongated neural outgrowth with less or no branching compared to C17.2 cells (Fig. 1C). To further investigate whether the radial-like unbranched neural extensions observed in FAS-treated NSCs were of neuronal origin, βIII-tubulin immunostaining was used. A supplementary figure contains information that revealed low βIII-tubulin expression in FAS-treated NSCs compared to C17.2 cells (Supplementary Fig. 2). βIII-tubulin expression showed a moderate increase in NSC neurite outgrowth by day 4 (Supplementary Fig. 2A–B), suggesting the majority of NSCs after fasudil treatment did not produce neuronal-like outgrowth but rather radial-like projections. By contrast, C17.2 showed stronger βIII-tubulin immunoreactivity with significant increase on day 2 and day 4 with FAS medium (Supplementary Fig. 2C–D).

3.2. Fasudil increases the expression of GFAP in postnatal NSCs

To further investigate changes observed *in vitro* in response to FAS-based medium, expression of NSC markers Nestin and Sox2, glial marker GFAP, and neuronal marker βIII-Tubulin were analysed over the 4-day FAS treatment by immunostaining (Fig. 2). Undifferentiated day 0 postnatal NSCs showed moderate Nestin and strong Sox2 signal, and were rare of GFAP or βIII-Tubulin expression (Fig. 2A). Upon FAS-treatment, there was a striking loss of nestin signal, and a significant increase in Sox2 detection in day 2 and day 4 (all compared to day 0 control) (Fig. 2B). FAS-treated NSCs also displayed significantly higher levels of GFAP expression on day 2 and day 4 compared to untreated control (Fig. 2B), while βIII-Tubulin signal, which was generally low, was reduced on day 2 but significantly increased by day 4 FAS-treatment. Taken together these results hinted that fasudil promoted gliogenesis of NSCs by increasing the expression of GFAP and Sox2 (markers of proliferating NSCs and reactive astrocytes) with concomitant reduction in Nestin and low βIII-Tubulin expression (markers of neuronal progenitors and early neural lineage, respectively).

Supplementary Fig. 3 shows the diverse effect of fasudil on C17.2 cells while Supplementary Figs. 4 and 5 show RT-PCR results of tested neural markers and immunohistochemistry of overgrown cultures respectively, complementing the gliogenic effect of fasudil on primary NSCs (Supplementary Figs. 3–5). In contrast to NSCs, fasudil treatment of C17.2 cells promoted the appearance of βIII-Tubulin-positive cells (Supplementary Fig. 3). Nestin signal was low in these cells but showed a significant increase at day 2 and day 4 (Supplementary Fig. 3B). This was accompanied by a moderate decrease in Sox2 detection on day 4 (Supplementary Fig. 3B). GFAP expression was observed to be weak throughout the treatment course. This suggests that fasudil promoted neuronal rather than glial lineage differentiation in C17.2 cells.

RT-PCR performed to complement the immunodetection data confirmed the trends observed. Accordingly, FAS-treated NSCs showed significant increases in *sox2* and *GFAP* mRNA (Supplementary Fig. 4A–B) while Fas treated C17.2 showed a moderate decrease in *sox2* and a significant increase in *βIII-tubulin* (Supplementary Fig. 4C–D).

We then compared the GFAP and βIII-Tubulin expression of day 2 and day 4 undifferentiated controls with FAS-treated NSCs and C17.2 cells (Supplementary Fig. 5). Day 2 FAS-treated NSCs showed higher levels of GFAP signal compared to all untreated controls, while βIII-Tubulin was always detected at low levels (Supplementary Fig. 5A–B). FAS-treated C17.2 showed very low levels of GFAP when compared to untreated controls in contrast to βIII-Tubulin expression which showed high level signals at both FAS-treated as well as overgrown cultures (Supplementary Fig. 5C–D). This shows that FAS-treated samples differentiated in a unique manner different from that of spontaneous differentiation of overgrown cultures *in vitro*.

3.3. Fasudil medium promoted radial interkinetic nuclear-like migration of postnatal NSCs

In order to further analyse the phenotypic changes in NSCs treated with FAS-based medium, the dynamics and migratory properties of the cells in culture were monitored by time-lapse microscopy. In the mammalian brain, migrating NSCs are known to express GFAP and show radial-like morphology (Malatesta et al., 2008; Doetsch et al., 1999; Kulikova et al., 2011; Del Bene, 2011; Spear and Erickson, 2012a). Radial glia populations display INM (interkinetic nuclear movement), a distinct migration pattern of the cell body along the radial-bidirectional cytoplasmic elongation, between the basal and apical layer of ventricular zone (Spear and Erickson, 2012a, Spear and Erickson, 2012b).

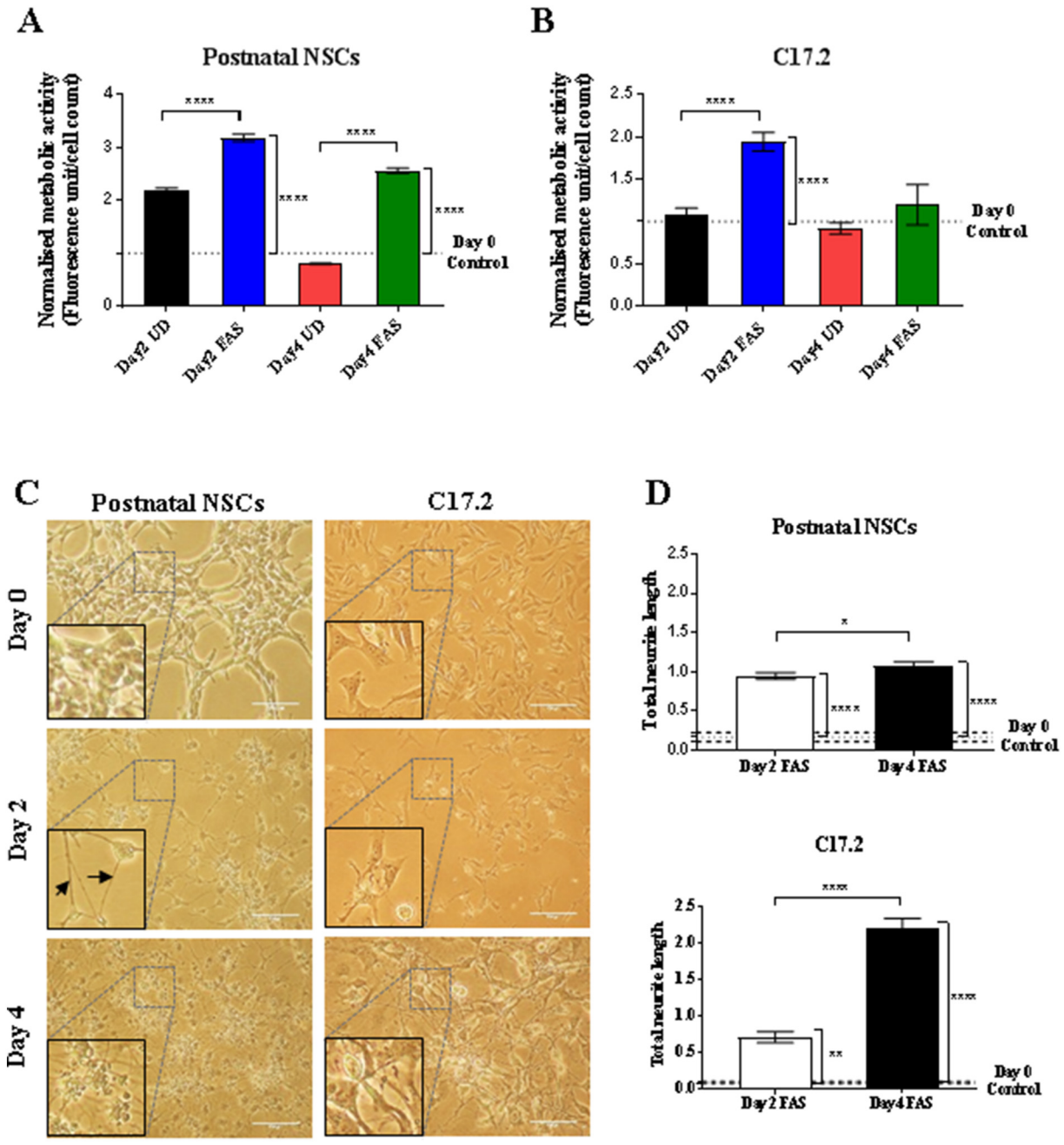

Fig. 1. Change in metabolic activity and neurite outgrowth upon FAS treatment. (A–B) Normalised metabolic activity measurements of postnatal NSCs (A) and C17.2 (B) cultures at 2 and 4 days of treatment with 100 μM FAS. All sample have been normalised to day 0 undifferentiated samples (dotted line). (C–D) Changes in neurite outgrowth upon FAS treatment analysed by brightfield images (C), with corresponding image analysis of neurite length of NSCs and C17.2 (D). Zoomed in boxes in (C) show details at higher magnification. Arrows show the radial-like morphology of cells. Scale bar: 250 μm. Statistical significance: *$p < 0.05$.

When postnatal NSC cultures were monitored under FAS-based treatment, NSCs were observed to form denser colonies and exhibited a radial-like migratory pattern suggestive of INM by day 2 (Fig. 3A). Notably, there was a significant increase in trackable migratory cells (B-E type) by day 4 (Fig. 3B). Supplementary video files show the radial-like movement of NSCs after FAS-treatment (Supplementary Videos 1–2). C17.2 cells showed a significant increase in trackable migratory cells both day 2 and day 4, however most C17.2 cells showed a tangential migratory pattern on day 2 of FAS treatment (Fig. 3A), displaying a 'crawling' behavior with short extentions. Additional video files show the migrational behaviour by C17.2 cells (Supplementary Video 3). The proportion of cells undergoing division (S-S type) significantly decreased in all FAS-medium samples compared to their day 0 counterparts (Fig. 3C), indicating FAS medium reduced the percentage of dividing cells or delayed the cell division. This suggested that, exposure to FAS medium promoted a more radial-like migratory phentype

Fig. 2. Marker expression analysis in postanatal NSCs exposed to fasudil. (A) Immunofluorescence images showing the expression of Nestin (green), Sox2 (red), GFAP (green) and βIII-tubulin (green) in undifferentiated day 0 and FAS-treated postnatal NSCs at day 2and day 4. DAPI used as nuclear counterstain (blue). (B) Corresponding signal quantitation using image analysis (dotted line is day 0). Scale bar 250 μm. *$p \leq 0.05$.

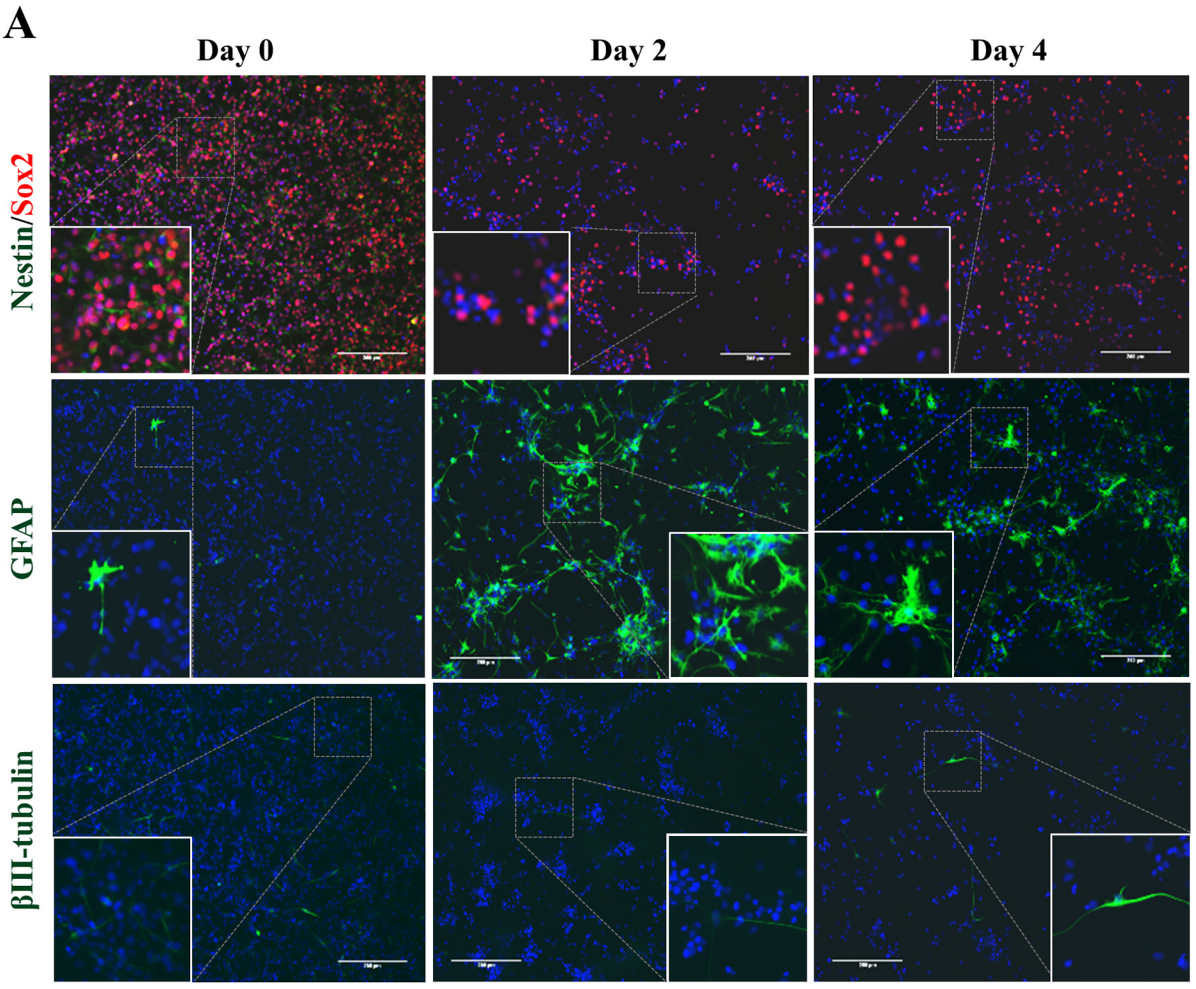
A
Day 0
Day 2
Day 4
Nestin/Sox2
GFAP
βIII-tubulin

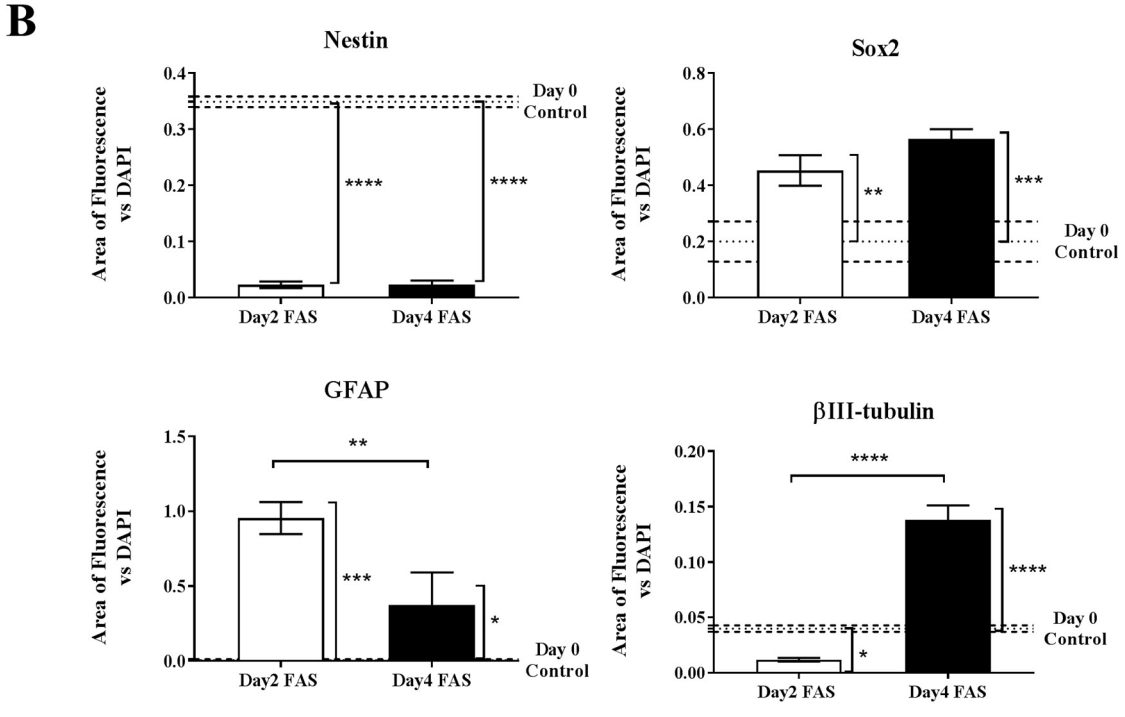
B
Nestin
Sox2
GFAP
βIII-tubulin
Area of Fluorescence vs DAPI
Day 0 Control
Day2 FAS
Day4 FAS
****
**
***
*

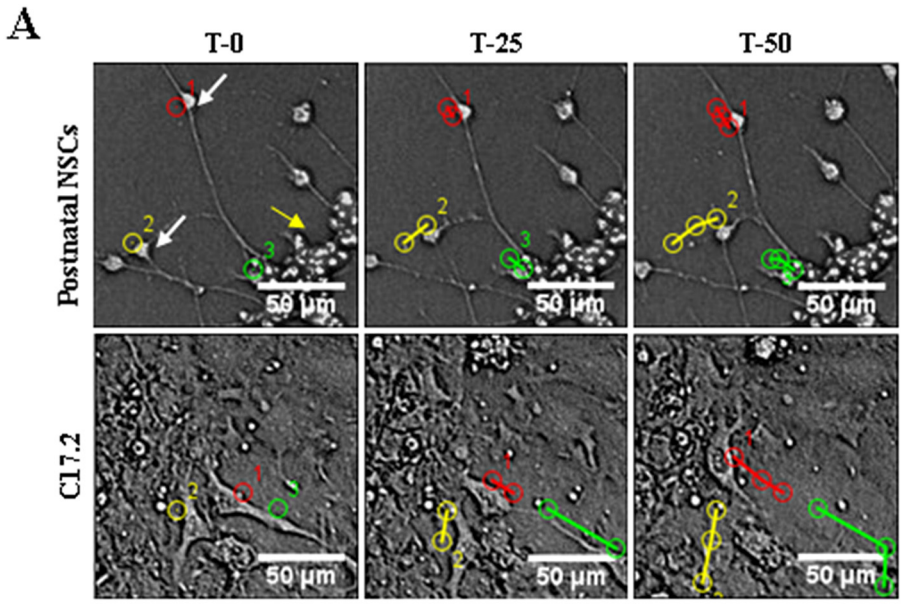
A
T-0
T-25
T-50
Postnatal NSCs
C17.2
50 µm

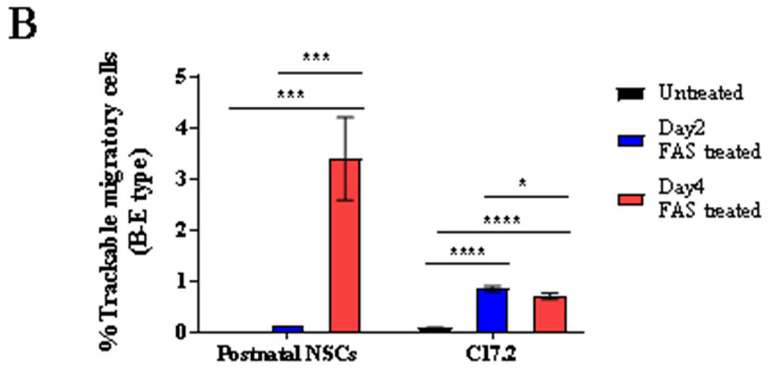
B
% Trackable migratory cells (B-E type)
Postnatal NSCs
C17.2
Untreated
Day2 FAS treated
Day4 FAS treated

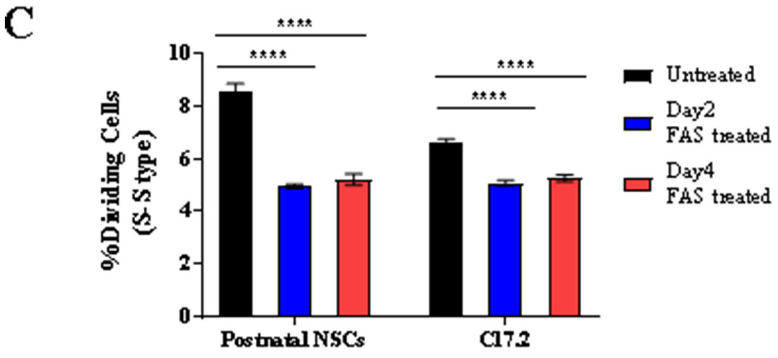
C
%Dividing Cells (S-S type)
Postnatal NSCs
C17.2
Untreated
Day2 FAS treated
Day4 FAS treated

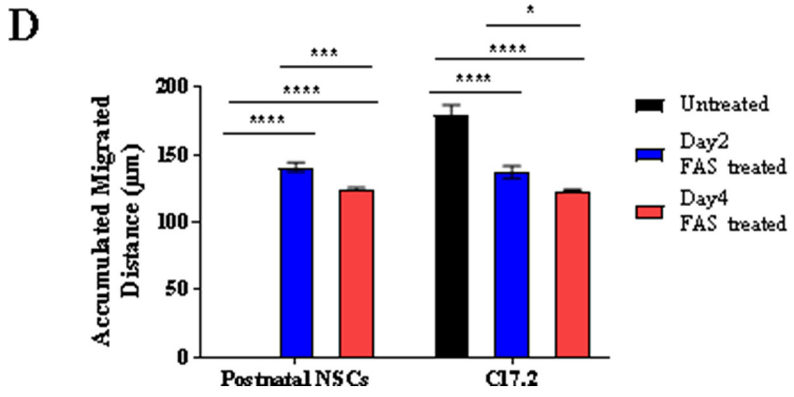
D
Accumulated Migrated Distance (µm)
Postnatal NSCs
C17.2
Untreated
Day2 FAS treated
Day4 FAS treated

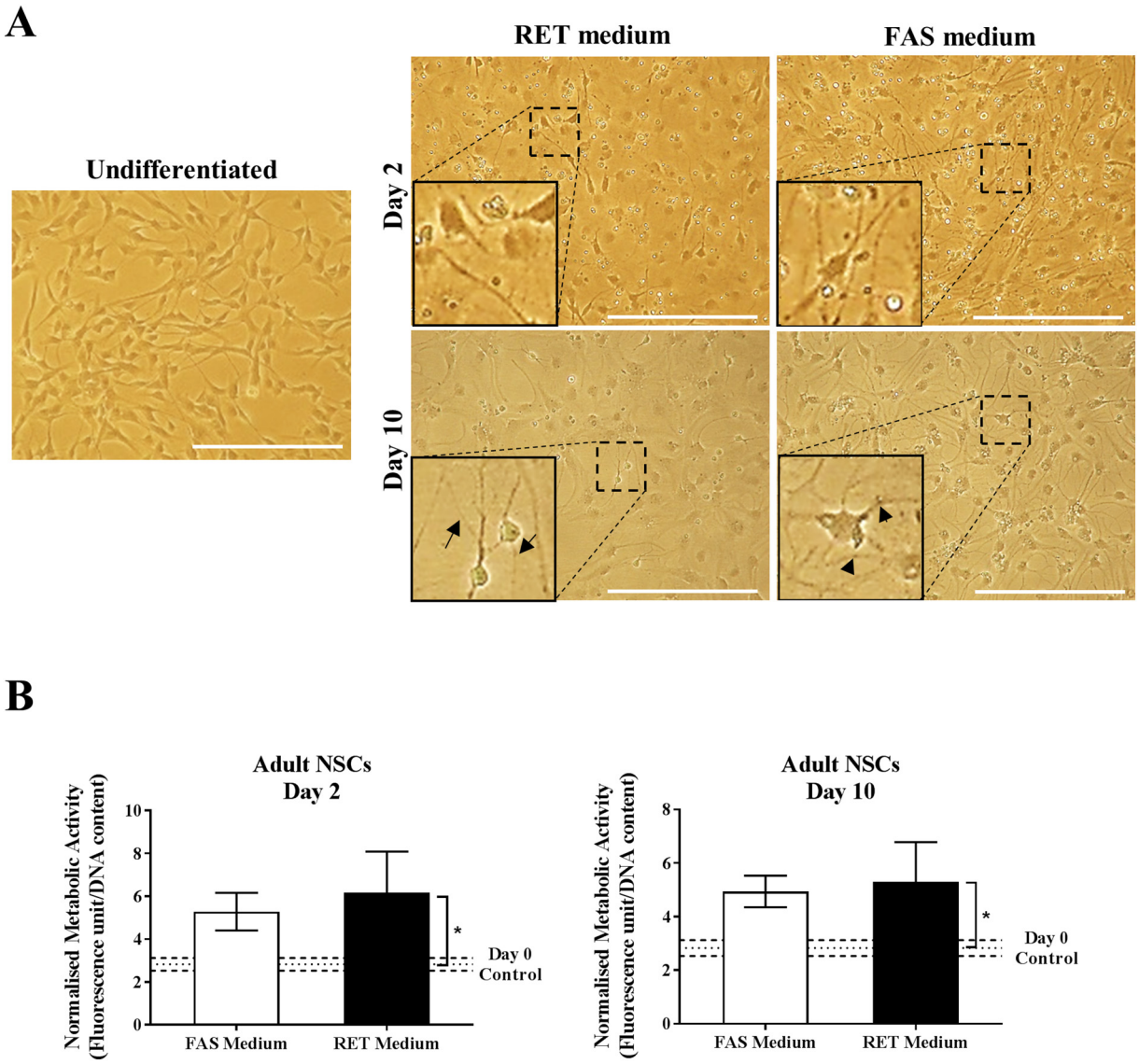

Fig. 4. Morphological and metabolic response of adult NSCs during RET- and FAS-differentiation on day 2 and day 10. (A) Morphological changes- arrows show the branching neurites in RET-treated adult NSCs *vs* flattened radial-like outgrowth in FAS-treated adult NSCs at day 10. Scale bar 250 μm. (B) Metabolic activity normalised to DNA content (dotted line is day 0). *$p < 0.05$.

in postnatal NSCs, different from the predominantly tangential-like migratory phenotype observed in treated C17.2 cells.

Finally, the total accumulated distance travelled by the non-dividing migratory cells in NSCs under FAS medium was found to rise sharply compared to day 0 control (Fig. 3D), while for C17.2 cells, the distance travelled under FAS medium was significantly lower than its day 0 control (Fig. 3D).

3.4. Fasudil-based differentiation compared to standard retinoid-based differentiation

Adult NSCs are more restricted in terms of differentiation and migration than embryonic and early postnatal NSCs (Obernier et al., 2014). In order to determine how FAS treatment may affect adult NSCs in culture and to compare its efficiency to that of conventional neuronal differentiating protocols involving a retinoic acid analogue (RET), adult NSCs were treated *in vitro* with both FAS-based and RET-based media for 10 days and monitored for metabolic and differentiation responses (Fig. 4). Both differentiation conditions were associated with rapid changes in cell morphology. By day 10, NSCs in RET medium showed mature neuronal morphologies with branched dendrites while NSCs in FAS medium showed flat morphological properties with less branching (Fig. 4A). There was no significant difference in cellular metabolic activity between the FAS-based and the RET-based conditions at day 2 and day 10 (Fig. 4B). Also, there was no significant reduction in metabolic activity in both FAS- and RET- differentiation compared to day 0 undifferentiated controls (Fig. 4B).

Based on these observations, NSC marker analysis was performed to evaluate potential phenotypic differences under the two differentiation regimes on day 10 *in vitro*. A supplementary figure contains

Fig. 3. Comparative time-lapse analysis of postnatal NSCs and C17.2 cells upon treatment with FAS medium. (A) Morphological changes of postnatal NSCs and C17.2 cells *in vitro*. Example of nucleo-kinetic locomotion of day 2 treated NSCs and tangential locomotion of day 2 treated C17.2 cells. T0, T25, T50 represent sequential time-points. Red, green and yellow markings represent the tracking of three independent cells in the images. White arrows show the radial-like morphology of cells. The yellow arrow shows the denser colony formed during FAS differentiation of NSCs. Scale bar 50 μm. (B) Percentage of trackable migratory cells (B-E type) in NSCs and C17.2 samples. (C) Percentage of dividing cells (S-S type) tracked in postnatal NSCs and C17.2 samples. (D) Quantitative analysis showing the total distance migrated by postnatal NSCs and C17.2 cells treated with FAS medium *vs.* undifferentiated cells. *$p < 0.05$.

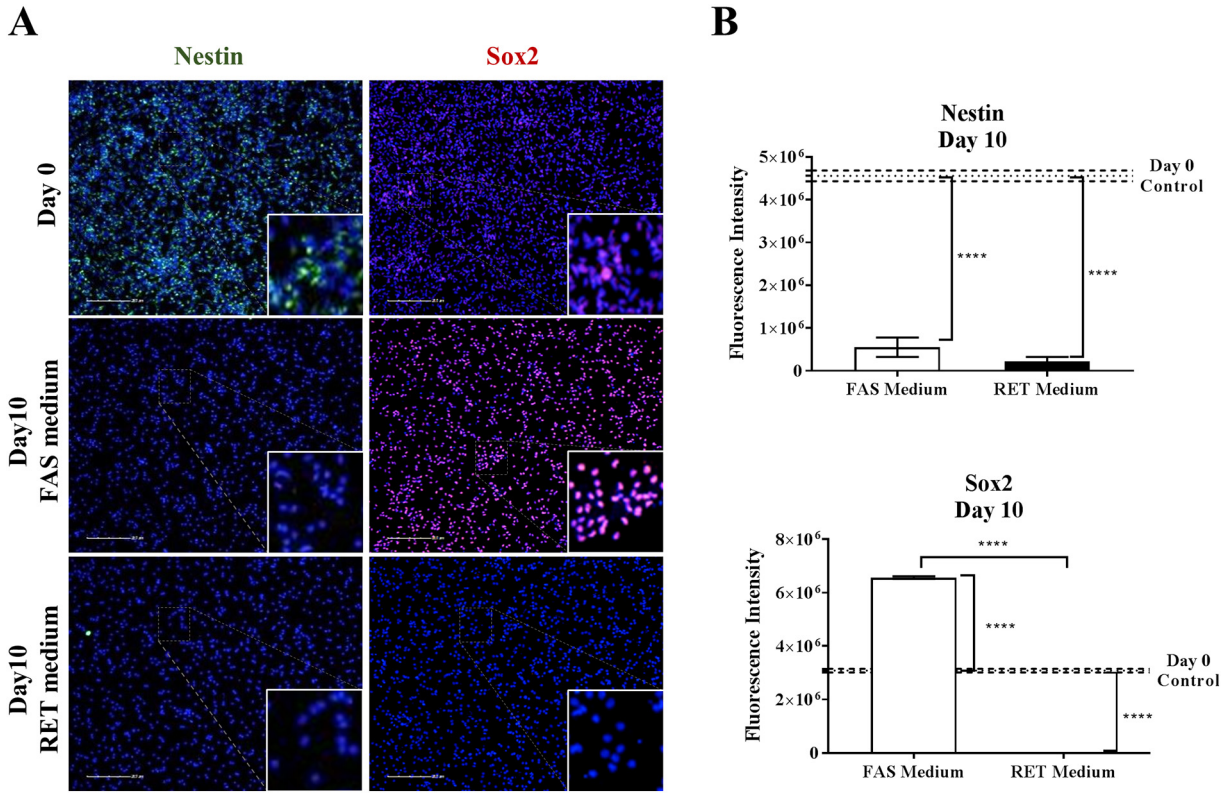

Fig. 5. Nestin and Sox2 expression in adult NSCs under FAS- and RET-differentiation protocols. (A) Nestin (green) and Sox2 (red) immunostaining at day 0 and day 10 of treatment and (B) corresponding image quantitation analysis (dotted line is day 0). DAPI used as nuclear counterstain (blue). Scale bar 200 μm. *$p < 0.05$.

the immunohistochemistry results for day 2 of NSC differentiation (Supplementary Fig. 6). Analysis of NSC marker expression indicated that both protocols equally reduced the expression of Nestin at day 10 (Fig. 5A–B). RET medium produced a marked reduction of Sox2 expression by day 10, while FAS medium increased the expression of Sox2 on both day 2 (Supplementary Fig. 6A–B) and day 10 (Fig. 5C–D).

3.5. Divergent differentiation responses of adult NSC under FAS- and RET-based conditions

Further analysis of lineage markers GFAP, βIII-Tubulin, S100b and DCX immunodetection was carried out to refine the phenotypic differences between the two treated NSC populations (Fig. 6 and Supplementary Fig. 7A–B). While GFAP expression increased in both FAS and RET treatments, cells under FAS medium displayed significantly higher expression by day 10, with an elongated radial-like morphology that was not observed in cells grown in RET medium (Fig. 6A–B). Expression of the neuronal marker βIII-Tubulin showed significant reduction in FAS medium, in contrast to the RET condition where multiple βIII-Tubulin positive neurons were observed (Fig. 6A–B). Adult NSCs were further stained for S100b and DCX, markers for mature astrocytes and migrating neuroblasts, respectively. While S100b expression was increased to comparable levels in both treatments, expression of the neuronal marker DCX was only detected in RET medium (Fig. 6A–B). qPCR analysis of these markers at day 10 (Fig. 7) confirmed transcriptional changes for *nestin*, *sox2*, *GFAP* and *βIII-tubulin* during FAS- and RET-based differentiation in line with the protein detection results, emphasizing the divergent effect of these 2 treatments on *sox2* and *βIII-tubulin* expression in NSCs. A supplementary figure contains the immunohistochemistry and qPCR results for day 2 of NSC differentiation (Supplementary Fig. 7).

4. Discussion

Fasudil is a ROCK inhibitor that has been shown to alleviate symptoms from a range of CNS disorders (Chen et al., 2013). Fasudil has been reported to improve stroke protection and blood flow after cerebral ischaemia by increasing NO (nitric oxide) production and eNOS (endothelium-derived NO synthase) expression (Rikitake et al., 2005). In experimental autoimmune encephalomyelitis, fasudil has been shown to delay the onset and severity of the disease by shifting microglia to an anti-inflammatory M2 phenotype that promotes tissue repair (Hou et al., 2012). Moreover, studies have suggested that fasudil can protect neurons and mobilize NSCs in *in vitro* ischaemic models by activating astrocyte secretion of granulocyte-colony stimulating factor (G-CSF) and inhibiting glutamate induced neurotoxicity (Ding et al., 2010; Huang et al., 2009; Yamashita et al., 2007). Recently, it has been shown that fasudil can mobilize endogenous NSCs *in vivo* and differentiate the C17.2 neural progenitor cell line *in vitro* (Ding et al., 2010; Chen et al., 2015). Taken together, these studies suggested a role for fasudil in NSC response and neurogenesis.

The use of fasudil has been reported in a variety of established neural and tumor cell lines at different concentrations (Compagnucci et al., 2016; Ding et al., 2010; Chen et al., 2015; Huang et al., 2009; Yamashita et al., 2007; Tonges et al., 2012; Tatenhorst et al., 2016; Tilson et al., 2015; Roloff et al., 2015; Takata et al., 2013; Deng et al., 2010; Lingor et al., 2007). Recently, C17.2 cerebellar progenitor cell line was used to study the differentiation effect of fasudil (Chen et al., 2015). It was shown that the differentiation was most rapid when a concentration of 100 μM FAS was used, which resulted in the production of neuronal cells expressing DCX (Chen et al., 2015). Using the same concentration, we showed that fasudil can differentiate C17.2 cells into βIII-tubulin neuronal cells, thereby confirming its effect. Interestingly, the differentiation effect of fasudil on primary NSCs had not so far been investigated. A previous study investigating the inhibitory effect of Rho-

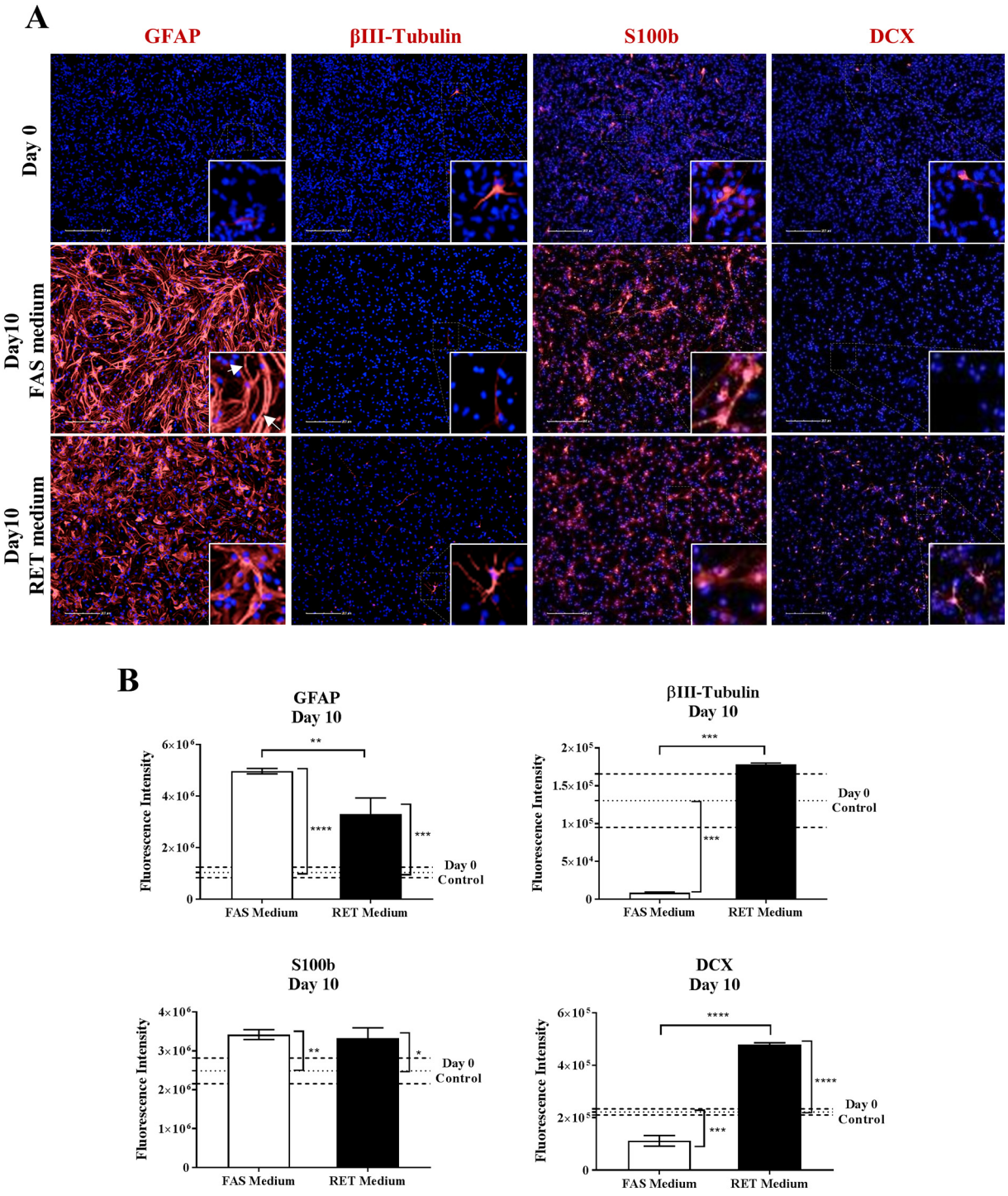

Fig. 6. GFAP, βIII-tubulin, s100b and DCX expression (red) in adult NSCs under FAS- and RET-differentiation protocols. (A) Immunofluorescence images at day 0 and day 10 of treatment (arrows indicate elongated radial-like neural outgrowth in GFAP positive cells) and (B) corresponding image quantitation analysis (dotted line is day 0). DAPI used as nuclear counterstain (blue). Scale bar 200 μm. *$p \leq 0.05$.

kinase on an *in vitro* model of Parkinson's disease reported 100 μM FAS to be toxic to primary midbrain neurons by reducing their cell number (Tonges et al., 2012), suggesting primary neural cells may be sensitive to this concentration of fasudil. Here however, we did not observe significant signs of reduced viability or impaired metabolic activity, indicating the dose of 100 μM FAS did not compromise the integrity of primary NSC cultures.

Fasudil treatment was observed to push the primary NSCs towards a gliogenic phenotype with radial-like properties. Radial glial NSCs present during development and radial glia-like NSCs present in the adult mammalian brain have shown potential to form neurons *in vivo* that integrate within the surrounding brain tissue and provide functional support during development, adult neurogenesis and tissue damage (Bignami and Dahl, 1974, Doetsch et al., 1999, Campbell and Gotz, 2002, Hutton and Pevny, 2011, Götz et al., 2015, Faiz et al., 2015). Upon proliferation and prior to differentiation, these cells are reported to express the markers GFAP and Sox2 (Bignami and Dahl, 1974, Doetsch et al., 1999, Campbell and Gotz, 2002, Hutton and Pevny, 2011, Götz et al., 2015). Here, we show that the differentiation of primary NSCs in the presence of fasudil lead to a loss of Nestin expression

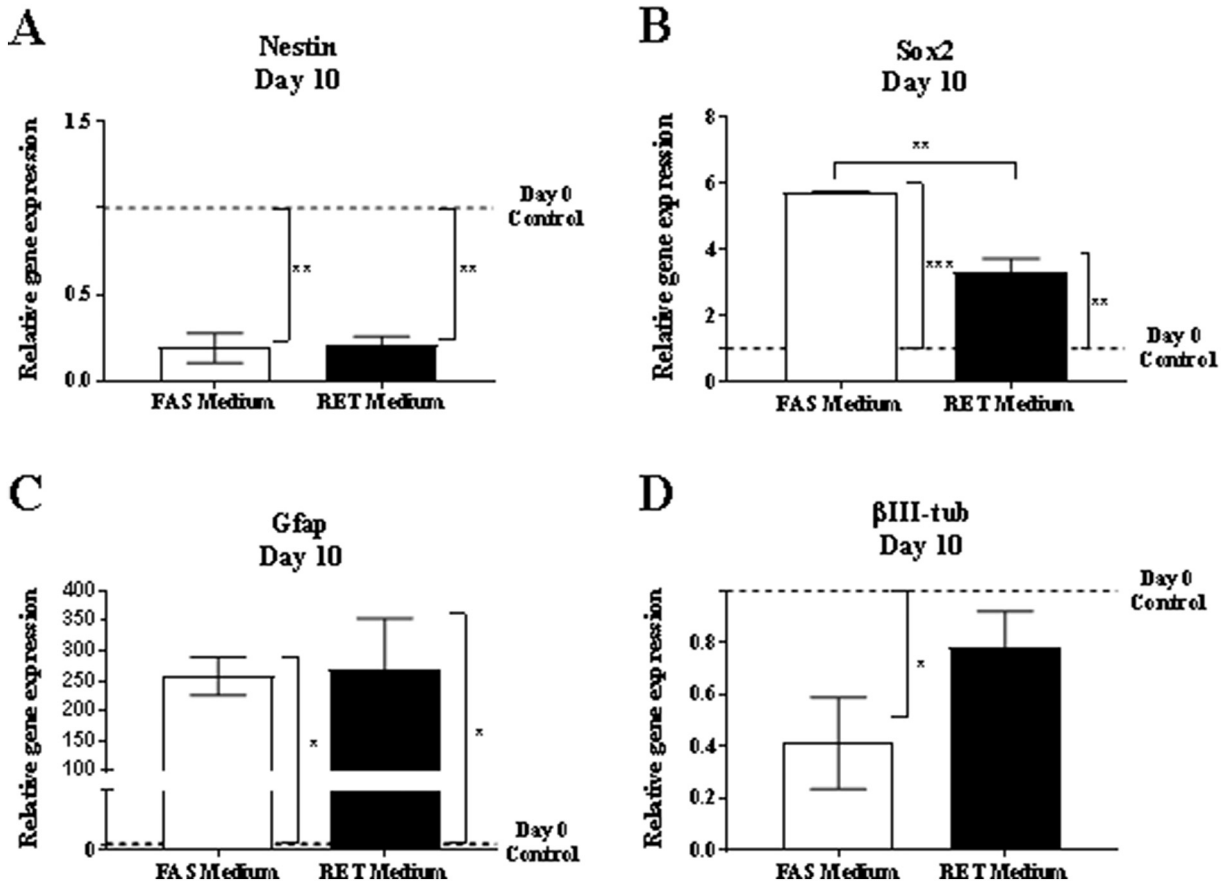

Fig. 7. qPCR analysis of adult NSCs in FAS- and RET-based medium on day 10 of differentiation under FAS- and RET- differentiation protocols for *Nestin*, *Sox2*, *GFAP* and *βIII-tub* (dotted line is day 0). *$p < 0.05$.

and an increase in Sox2 and GFAP expression in postnatal and adult NSCs *in vitro*. NSCs *in vivo* have the ability to migrate during CNS development or in the adult brain in response to injury. When monitoring the migratory pattern of primary postnatal NSCs, an increase in migratory behaviour was observed in response to FAS medium. At the early stage of treatment, postnatal NSCs exhibited INM, with the characteristic movement of cell soma along radial extensions, a phenotype associated with radial glia known to modulate various stages of neural development including epithelial remodelling, maintenance of epithelial structure and polarity, and neural proliferation and differentiation (Spear and Erickson, 2012a, Spear and Erickson, 2012b, Glaser and Brüstle, 2005). FAS-treatment thus induced NSCs to display gene expression and migratory characteristics of radial-glial progenitors *in vitro*, and promoted a gliogenic phenotype. This protocol produced minimal neurogenic response, indicating the potential of fasudil as a pro-neuroglial agent. Protein and transcript detection showed rare expression of neuronal markers upon treatment, in contrast to the retinoid-based neuronal differentiation protocol, which induced the expression of βIII-tubulin and DCX in culture.

We observed an increase of Sox2 expression by day 10 of FAS-treatment, which contrasted with the response to RET-treatment. Sox2 plays a vital role in NSC proliferation and regulation (Hutton and Pevny, 2011; Cimadamore et al., 2013; Episkopou, 2005), and has been reported to inhibit neuronal differentiation in the mouse neocortex, unless the Notch pathway is blocked (Bani-Yaghoub et al., 2006). A recent study has shown that overexpression of Sox2 reduced the number of MAP2 positive neurons in human pluripotent NT2/D1 cells *in vitro* (Klajn et al., 2014), while astrocytes retained Sox2 expression along with GFAP. It is thus possible to speculate that fasudil may promote gliogenesis in NSCs by increasing Sox2 expression. Recently, fasudil has been suggested to be involved in modulating major NSC signaling pathways including Notch and NF-kB (Chen et al., 2015; Okamoto et al., 2010). Notch signaling acts as a molecular switch in regulating neural stem cell (NSC) lineage determination *in vivo* and *in vitro*, by promoting gliogenesis, self-renewal of NSCs, and inhibiting neuronal differentiation (Zhou et al., 2010). Fasudil has also been known to modulate NFκB by inhibiting IL-1–induced activation of NFκB in a rat model of rheumatoid arthritis (Okamoto et al., 2010; Sato et al., 1998). In NSCs, inhibition of NF-kB has been shown to increase expression of NSC markers Nestin and Sox2 while inhibiting neuronal differentiation *in vitro* (Zhang et al., 2012). It will thus be of interest to determine whether fasudil's effect on Sox2 expression in primary NSCs may thus be mediated through its effects on the Notch and/or NFκB pathways.

5. Conclusion

The present study explored the effects of fasudil on NSC cultures derived from mouse SVZ. Fasudil was observed to promote neural outgrowth of primary neural stem cells. Immunodetection and RT-PCR have provided evidence that fasudil treatment promotes enhanced gliogenesis of postnatal NSCs, and real-time imaging showed that fasudil treatment promotes radial-like inter-kinetic nuclear movement in postnatal NSCs. A similar effect was observed in adult NSCs, as fasudil promoted gliogenesis of adult NSCs with increase in Sox2 expression and absence of neuronal markers βIII-tubulin and DCX. These results provide the first evidence that fasudil can be used for the treatment of primary NSCs in culture with no toxicity, and can promote differentiation towards a gliogenic phenotype, thus contributing to the development of *in vitro* models of neural differentiation.

This study shows that fasudil treatment applied to primary NSCs provides an efficient model to analyse the key aspects of *in vivo* gliogenesis. In addition to radial glia, reactive astrocytes in the adult brain also express GFAP and Sox2 and show proliferative and migratory response towards injury (Götz et al., 2015; Buffo et al., 2008). Here we report that fasudil-treated primary NSCs share the expression and morphological patterns of radial as well as reactive gliosis, two fundamental aspects of *in vivo* gliogenesis. GFAP and S100b detection highlighted the gliogenic differentiation of NSCs, and future characterisation of this newly identified FAS-mediated response will help determine whether fasudil can promote the appearance of specific glial subtypes such as oligodendrocytes.

Fasudil-treated NSCs can be used as a model to study INM of NSCs *in vitro*, providing a rapid and efficient procedure compared to tissue slice culture and *in vivo* studies (Kulikova et al., 2011; Tsai et al., 2010; Marin et al., 2010). Future applications could include the molecular characterisation of INM processes by combining this method with the recently published cell cycle staging protocol using high-content screening (Del Bene, 2011; Roukos et al., 2015; Cecchini et al., 2012).

Our results also suggest that fasudil's target, the Rho/ROCK cascade, could be an important NSC regulatory pathway. Furthermore, fasudil has also been suggested to inhibit other functional kinases including protein kinase N1 (PKN1), protein kinase C (PKC), cyclic nucleotide dependant protein kinases (PKA and PKG) and Ca^{2+}/calmodulin dependant myosin light chain kinase (MLCK) in a concentration dependant manner, resulting in off-target effects with respect to ROCK inhibition (Asano et al., 1989; Fajardo et al., 2014; Scott, 1991; Dugan et al., 1999). It will therefore be necessary to investigate to what extent ROCK inhibition might be the main mechanism for the fasudil-mediated gliogenic differentiation observed in NSCs, in order to further exploit this pharmacological pathway and its potential to regulate and control stem cell populations for CNS repair strategies.

Supplementary data to this article can be found online at https://doi.org/10.1016/j.scr.2018.02.001.

Funding

This research did not receive any specific grant from funding agencies in the public, commercial, or not-for-profit sectors.

Acknowledgements

We are grateful to Katarzyna Lis-Slimak (School of Medicine, U. of Nottingham) for her expert help with the Operetta High-Content Imaging system. We thank Rebecca Trueman (School of Life Sciences, U. of Nottingham), Anaid Lugo-Leija and Nigel De Melo (School of Medicine, U. of Nottingham), and Inchirah Adala (School of Pharmacy, U. of Nottingham) for their invaluable comments. A kind donation from R. Jones in the memory of A. Stacey is gratefully acknowledged.

References

Asano, T., Suzuki, T., Tsuchiya, M., Satoh, S., Ikegaki, I., Shibuya, M., Suzuki, Y., Hidaka, H., 1989. Vasodilator actions of HA1077 in vitro and in vivo putatively mediated by the inhibition of protein kinase. Br. J. Pharmacol. 98, 1091–1100.

Baba, H., Tanoue, Y., Maeda, T., Kobayashi, M., Oda, S., Tominaga, R., 2010. Protective effects of cold spinoplegia with fasudil against ischemic spinal cord injury in rabbits. J. Vasc. Surg. 51, 445–452.

Bani-Yaghoub, M., Tremblay, R.G., Lei, J.X., Zhang, D., Zurakowski, B., Sandhu, J.K., Smith, B., Ribecco-Lutkiewicz, M., Kennedy, J., Walker, P.R., 2006. Role of Sox2 in the development of the mouse neocortex. Dev. Biol. 295, 52–66.

Bignami, A., Dahl, D., 1974. Astrocyte-specific protein and radial glia in the cerebral cortex of newborn rat. Nature 252, 55–56.

Boyce-Rustay, J.M., Simler, G.H., McGaraughty, S., Chu, K.L., Wensink, E.J., Vasudevan, A., Honore, P., 2010. Characterization of Fasudil in preclinical models of pain. J. Pain 11, 941–949.

Buffo, A., Rite, I., Tripathi, P., Lepier, A., Colak, D., Horn, A.P., Mori, T., Gotz, M., 2008. Origin and progeny of reactive gliosis: a source of multipotent cells in the injured brain. Proc. Natl. Acad. Sci. U. S. A. 105, 3581–3586.

Campbell, K., Gotz, M., 2002. Radial glia: multi-purpose cells for vertebrate brain development. Trends Neurosci. 25, 235–238.

Cecchini, M.J., Amiri, M., Dick, F.A., 2012. Analysis of cell cycle position in mammalian cells. J. Vis. Exp. 59 pii: 3491.

Chen, M., Liu, A., Ouyang, Y., Huang, Y., Chao, X., Pi, R., 2013. Fasudil and its analogs: a new powerful weapon in the long war against central nervous system disorders? Expert Opin. Investig. Drugs 22, 537–550.

Chen, S., Luo, M., Zhao, Y., Zhang, Y., He, M., Cai, W., Liu, A., 2015. Fasudil stimulates neurite outgrowth and promotes differentiation in C17.2 neural stem cells by modulating notch signalling but not autophagy. Cell. Physiol. Biochem. 36, 531–541.

Cimadamore, F., Amador-Arjona, A., Chen, C., Huang, C.-T., Terskikh, A.V., 2013. SOX2–LIN28/let-7 pathway regulates proliferation and neurogenesis in neural precursors. Proc. Natl. Acad. Sci. 110, E3017–E3026.

Compagnucci, C., Barresi, S., Petrini, S., Billuart, P., Piccini, G., Chiurazzi, P., Alfieri, P., Bertini, E., Zanni, G., 2016. Rho kinase inhibition is essential during in vitro neurogenesis and promotes phenotypic rescue of human induced pluripotent stem cell-derived neurons with oligophrenin-1 loss of function. Stem Cells Transl. Med. 5, 860–869.

Del Bene, F., 2011. Interkinetic nuclear migration: cell cycle on the move. EMBO J. 30, 1676–1677.

Deng, L., Li, G., Li, R., Liu, Q., He, Q., Zhang, J., 2010. Rho-kinase inhibitor, fasudil, suppresses glioblastoma cell line progression in vitro and in vivo. Cancer Biol. Ther. 9, 875–884.

Ding, J., Li, Q.Y., Yu, J.Z., Wang, X., Sun, C.H., Lu, C.Z., Xiao, B.G., 2010. Fasudil, a rho kinase inhibitor, drives mobilization of adult neural stem cells after hypoxia/reoxygenation injury in mice. Mol. Cell. Neurosci. 43, 201–208.

Doetsch, F., Caille, I., Lim, D.A., Garcia-Verdugo, J.M., Alvarez-Buylla, A., 1999. Subventricular zone astrocytes are neural stem cells in the adult mammalian brain. Cell 97, 703–716.

Dugan, L.L., Kim, J.S., Zhang, Y., Bart, R.D., Sun, Y., Holtzman, D.M., Gutmann, D.H., 1999. Differential effects of cAMP in neurons and astrocytes role of B-raf. J. Biol. Chem. 274, 25842–25848.

Episkopou, V., 2005. SOX2 functions in adult neural stem cells. Trends Neurosci. 28, 219–221.

Faiz, M., Sachewsky, N., Gascón, S., Bang, K.W.A., Cindi, M., Morshead, A. Nagy, 2015. Adult neural stem cells from the subventricular zone give rise to reactive astrocytes in the cortex after stroke. Cell Stem Cell 17, 624–634.

Fajardo, A.M., Piazza, G.A., Tinsley, H.N., 2014. The role of cyclic nucleotide signaling pathways in cancer: targets for prevention and treatment. Cancer 6, 436–458.

Glaser, T., Brüstle, O., 2005. Retinoic acid induction of ES-cell-derived neurons: the radial glia connection. Trends Neurosci. 28, 397–400.

Götz, M., Sirko, S., Beckers, J., Irmler, M., 2015. Reactive astrocytes as neural stem or progenitor cells: in vivo lineage, in vitro potential, and genome-wide expression analysis. Glia 63, 1452–1468.

Gu, H., Yu, S.P., Gutekunst, C.-A., Gross, R.E., Wei, L., 2013. Inhibition of the rho signaling pathway improves neurite outgrowth and neuronal differentiation of mouse neural stem cells. Int. J. Physiol. Pathophysiol. Pharmacol. 5, 11–20.

Hara, M., Takayasu, M., Watanabe, K., Noda, A., Takagi, T., Suzuki, Y., Yoshida, J., 2000. Protein kinase inhibition by fasudil hydrochloride promotes neurological recovery after spinal cord injury in rats. J. Neurosurg. Spine 93, 94–101.

Hou, S.W., Liu, C.Y., Li, Y.H., Yu, J.Z., Feng, L., Liu, Y.T., Guo, M.F., Xie, Y., Meng, J., Zhang, H.F., Xiao, B.G., Ma, C.G., 2012. Fasudil ameliorates disease progression in experimental autoimmune encephalomyelitis, acting possibly through antiinflammatory effect. CNS Neurosci. Therap. 18, 909–917.

Huang, L., Li, Q., Li, H., He, Z., Cheng, Z., Chen, J., Guo, L., 2009. Inhibition of intracellular Ca 2+ release by a Rho-kinase inhibitor for the treatment of ischemic damage in primary cultured rat hippocampal neurons. Eur. J. Pharmacol. 602, 238–244.

Hutton, S.R., Pevny, L.H., 2011. SOX2 expression levels distinguish between neural progenitor populations of the developing dorsal telencephalon. Dev. Biol. 352, 40–47.

Impellizzeri, D., Mazzon, E., Paterniti, I., Esposito, E., Cuzzocrea, S., 2012. Effect of fasudil, a selective inhibitor of Rho kinase activity, in the secondary injury associated with the experimental model of spinal cord trauma. J. Pharmacol. Exp. Ther. 343, 21–33.

Inan, S., Büyükafşar, K., 2008. Antiepileptic effects of two Rho-kinase inhibitors, Y-27632 and fasudil, in mice. Br. J. Pharmacol. 155, 44–51.

Jia, X.-f., Ye, F., Wang, Y.-b., Feng, D.-x., 2016. ROCK inhibition enhances neurite outgrowth in neural stem cells by upregulating YAP expression in vitro. Neural Regen. Res. 11, 983.

Klajn, A., Drakulic, D., Tosic, M., Pavkovic, Z., Schwirtlich, M., Stevanovic, M., 2014. SOX2 overexpression affects neural differentiation of human pluripotent NT2/D1 cells. Biochem. Mosc. 79, 1172–1182.

Kulikova, S., Abatis, M., Heng, C., Lelievre, V., 2011. Interkinetic nuclear migration. Cell Adhes. Migr. 5, 277–279.

Lingor, P., Teusch, N., Schwarz, K., Mueller, R., Mack, H., Bahr, M., Mueller, B.K., 2007. Inhibition of rho kinase (ROCK) increases neurite outgrowth on chondroitin sulphate proteoglycan in vitro and axonal regeneration in the adult optic nerve in vivo. J. Neurochem. 103, 181–189.

Liu, J., Gao, H.-y., Wang, X.-f., 2015. The role of the Rho/ROCK signaling pathway in inhibiting axonal regeneration in the central nervous system. Neural Regen. Res. 10, 1892–1896.

Malatesta, P., Appolloni, I., Calzolari, F., 2008. Radial glia and neural stem cells. Cell Tissue Res. 331, 165–178.

Marin, O., Valiente, M., Ge, X., Tsai, L.H., 2010. Guiding neuronal cell migrations. Cold Spring Harb. Perspect. Biol. 2, a001834.

Mueller, B.K., Mack, H., Teusch, N., 2005. Rho kinase, a promising drug target for neurological disorders. Nat. Rev. Drug Discov. 4, 387.

Nakamura, T., Matsui, T., Hosono, A., Okano, A., Fujisawa, N., Tsuchiya, T., Indo, M., Suzuki, Y., Oya, S., Chang, H.S., 2013. Beneficial effect of selective intra-arterial infusion of

fasudil hydrochloride as a treatment of symptomatic vasospasm following SAH. Acta Neurochir. Suppl. 115, 81–85.
Obernier, K., Tong, C.K., Alvarez-Buylla, A., 2014. Restricted nature of adult neural stem cells: re-evaluation of their potential for brain repair. Front. Neurosci. 8.
Okamoto, H., Yoshio, T., Kaneko, H., Yamanaka, H., 2010. Inhibition of NF-kappaB signaling by fasudil as a potential therapeutic strategy for rheumatoid arthritis. Arthritis Rheum. 62, 82–92.
Rikitake, Y., Kim, H.H., Huang, Z., Seto, M., Yano, K., Asano, T., Moskowitz, M.A., Liao, J.K., 2005. Inhibition of Rho kinase (ROCK) leads to increased cerebral blood flow and stroke protection. Stroke 36, 2251–2257.
Roloff, F., Scheiblich, H., Dewitz, C., Dempewolf, S., Stern, M., Bicker, G., 2015. Enhanced neurite outgrowth of human model (NT2) neurons by small-molecule inhibitors of Rho/ROCK signaling. PLoS One 10, e0118536.
Roukos, V., Pegoraro, G., Voss, T.C., Misteli, T., 2015. Cell cycle staging of individual cells by fluorescence microscopy. Nat. Protoc. 10, 334–348.
Sato, T., Asamitsu, K., Yang, J.P., Takahashi, N., Tetsuka, T., Yoneyama, A., Kanagawa, A., Okamoto, T., 1998. Inhibition of human immunodeficiency virus type 1 replication by a bioavailable serine/threonine kinase inhibitor, fasudil hydrochloride. AIDS Res. Hum. Retrovir. 14, 293–298.
Satoh, S., Takayasu, M., Kawasaki, K., Ikegaki, I., Hitomi, A., Yano, K., Shibuya, M., Asano, T., 2012. Antivasospastic effects of hydroxyfasudil, a Rho-kinase inhibitor, after subarachnoid hemorrhage. J. Pharmacol. Sci. 118, 92–98.
Scott, J.D., 1991. Cyclic nucleotide-dependent protein kinases. Pharmacol. Ther. 50, 123–145.
Shibuya, M., Suzuki, Y., Sugita, K., Saito, I., Sasaki, T., Takakura, K., Nagata, I., Kikuchi, H., Takemae, T., Hidaka, H., 1992. Effect of AT877 on cerebral vasospasm after aneurysmal subarachnoid hemorrhage: results of a prospective placebo-controlled double-blind trial. J. Neurosurg. 76, 571–577.
Spear, P.C., Erickson, C.A., 2012a. Interkinetic nuclear migration: a mysterious process in search of a function. Develop. Growth Differ. 54, 306–316.
Spear, P.C., Erickson, C.A., 2012b. Apical movement during interkinetic nuclear migration is a two-step process. Dev. Biol. 370, 33–41.
Takata, M., Tanaka, H., Kimura, M., Nagahara, Y., Tanaka, K., Kawasaki, K., Seto, M., Tsuruma, K., Shimazawa, M., Hara, H., 2013. Fasudil, a rho kinase inhibitor, limits motor neuron loss in experimental models of amyotrophic lateral sclerosis. Br. J. Pharmacol. 170, 341–351.
Tatenhorst, L., Eckermann, K., Dambeck, V., Fonseca-Ornelas, L., Walle, H., Lopes da Fonseca, T., Koch, J.C., Becker, S., Tonges, L., Bahr, M., Outeiro, T.F., Zweckstetter, M., Lingor, P., 2016. Fasudil attenuates aggregation of alpha-synuclein in models of Parkinson's disease. Acta Neuropathol. Commun. 4, 39.
Tilson, S.G., Haley, E.M., Triantafillu, U.L., Dozier, D.A., Langford, C.P., Gillespie, G.Y., Kim, Y., 2015. ROCK inhibition facilitates in vitro expansion of glioblastoma stem-like cells. PLoS One 10, e0132823.
Tonges, L., Frank, T., Tatenhorst, L., Saal, K.A., Koch, J.C., Szego, E.M., Bahr, M., Weishaupt, J. H., Lingor, P., 2012. Inhibition of rho kinase enhances survival of dopaminergic neurons and attenuates axonal loss in a mouse model of Parkinson's disease. Brain J. Neurol. 135, 3355–3370.
Tsai, J.-W., Lian, W.-N., Kemal, S., Kriegstein, A.R., Vallee, R.B., 2010. Kinesin 3 and cytoplasmic dynein mediate interkinetic nuclear migration in neural stem cells. Nat. Neurosci. 13, 1463–1471.
Villar-Cheda, B., Dominguez-Meijide, A., Joglar, B., Rodriguez-Perez, A.I., Guerra, M.J., Labandeira-Garcia, J.L., 2012. Involvement of microglial RhoA/rho-kinase pathway activation in the dopaminergic neuron death. Role of angiotensin via angiotensin type 1 receptors. Neurobiol. Dis. 47, 268–279.
Wang, Q.M., Stalker, T.J., Gong, Y., Rikitake, Y., Scalia, R., Liao, J.K., 2012. Inhibition of rho-kinase attenuates endothelial–leukocyte interaction during ischemia–reperfusion injury. Vasc. Med. 17, 379–385.
Yamashita, K., Kotani, Y., Nakajima, Y., Shimazawa, M., Yoshimura, S.-i., Nakashima, S., Iwama, T., Hara, H., 2007. Fasudil, a rho kinase (ROCK) inhibitor, protects against ischemic neuronal damage in vitro and in vivo by acting directly on neurons. Brain Res. 1154, 215–224.
Ying, H., Biroc, S.L., Li, W.W., Alicke, B., Xuan, J.A., Pagila, R., Ohashi, Y., Okada, T., Kamata, Y., Dinter, H., 2006. The rho kinase inhibitor fasudil inhibits tumor progression in human and rat tumor models. Mol. Cancer Ther. 5, 2158–2164.
Zhang, Y., Liu, J., Yao, S., Li, F., Xin, L., Lai, M., Bracchi-Ricard, V., Xu, H., Yen, W., Meng, W., Liu, S., Yang, L., Karmally, S., Liu, J., Zhu, H., Gordon, J., Khalili, K., Srinivasan, S., Bethea, J.R., Mo, X., Hu, W., 2012. Nuclear factor kappa B signaling initiates early differentiation of neural stem cells. Stem Cells (Dayton, Ohio) 30, 510–524.
Zhou, Z.D., Kumari, U., Xiao, Z.C., Tan, E.K., 2010. Notch as a molecular switch in neural stem cells. IUBMB Life 62, 618–623.